Project 1 for Complex Adaptive Systems

Vanessa Job
Department of Computer Science
University of New Mexico
vjob@unm.edu

Kellin Rumsey
Department of Mathematics and Statistics
University of New Mexico
knrumsey@unm.edu

***Abstract*—In this paper, we investigate the direction of causal information transfer from global to local scales and vice versa. As in previous work, we use a system of coupled logistic maps as a toy example of population growth. We explore the collective behavior which arises in a variety of forms for different values of a global coupling parameter. We utilize state-of-the-art estimation procedures to infer both top-down and bottom-up transfer entropies. Finally, we analyze these results as they pertain to global coupling, and attempt to uderstand their implications.**

I. Introduction

Evolution proceeds by emergence of new higher level entities. How information is stored and processed is a driver of this process [1]. For instance, the emergence of epigenetic inheritance provided a competitive advantage through diversification. In this paper, we look at the interaction between organisms as individual populations and organisms considered as a group of populations.

For individual populations, we assume birth rate, death rate, and carrying capacity are all fixed. Define k to be the carrying capacity of a population and n_t to be size of the population at time t. Then the size of the population at generation t is modeled by

$$n_{t+1} = (\text{birthrate} - \text{deathrate})(kn_t - n_t^2)/k \tag{1}$$

If we define the population size relative to the carrying capacity as $x_t = n_t/k$ and define the reproductive fitness $r = birthrate - deathrate$, then we get the following equation for x_t:

$$x_{t+1} = rx_t(1 - x_t), \qquad t = 0, 1, 2, \ldots. \tag{2}$$

This is the logistic map as defined in [3]. In what follows, we will refer to x_t as the population size, with the understanding that it will always be the ratio of the actual population size to the carrying capacity.

In [1], the authors investigate information flow between higher and lower levels of organization, between individuals of a population and the population considered as a whole. They study a model that consists of a population of individual populations and examine the direction of the causal information transfer, where "non-trivial collective behavior is associated with the degree to which local elements receive information from the global network." [1]

Their model, a lattice of globally coupled logistic maps, is used to investigate the circumstances under which nontrivial collective behavior occurs. Through the use of transfer entropy, they show the relationship between a global coupling parameter and direction of information flow. They also illustrate the relationship between these dynamics and the emergence of complex collective behavior of the populations.

In this paper, we seek to reproduce these results and to answer some additional questions. We will explore in detail the behavior of the mean-field as a function of global coupling strength and thus by direction of information flow. In addition, we will attempt to improve on the estimation of transfer entropy via the use of kernel density estimators (2A) and Kraskov's estimator (section 2D). Finally, we consider the direction of information as described by transfer entropy in the average case, rather than relying on making inferences from a single simulation.

II. Methods and Results

A. Sensitive Dependence on Initial Conditions

Depending on the value of the reproductive fitness r, the logistic map will generate a population size that is stable, periodic, or chaotic over time. The behavior of the logistic map can vary a great deal with small changes in x_0. This phenomenon is known as *sensitive dependence on initial conditions*, where small changes in the input lead to large changes in the output. In figure 1, we plot four times series showing population versus time for 50 time steps.

The mutual information measures the dependence of one random variable on another random variable. For two random variables X and Y, we define the mutual information to be

$$I(X, Y) = \sum_{y \in Y} \sum_{x \in X} p(x, y) \frac{\log p(x, y)}{\log p(x) \log p(y)} \tag{3}$$

When two random variables are independent, their mutual information is 0.

We first estimated the mutual information for the time series in figure 1(a) and figure 1(b) using binning. The mutual information for the periodic maps in figure 1(a) is 0.7522 and the mutual information for the chaotic maps is 0.0471. This makes sense because after $t = 13$, for the periodic maps, you

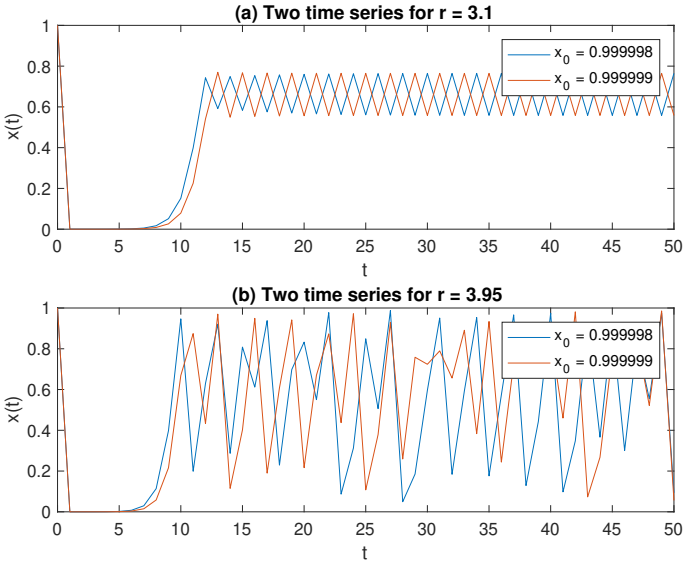

Fig. 1. Population growth over time showing sensitive dependence on initial conditions. The mutual information for the periodic map (a) is 0.7522. The mutual information for the chaotic map (b) is 0.0471.

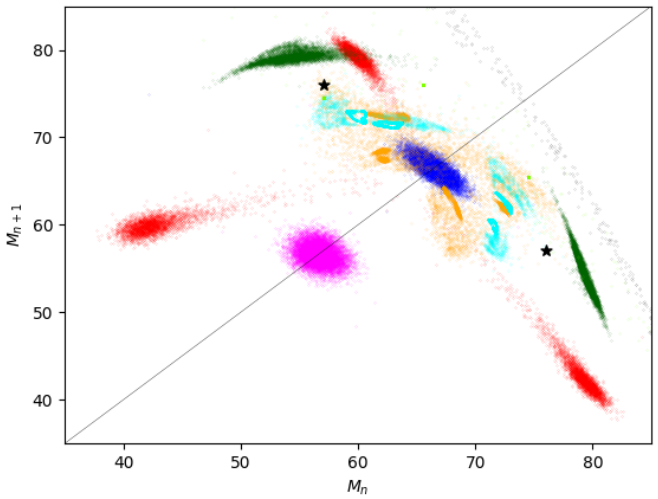

Fig. 2. Return map for selected values of the global coupling strength ϵ: $\epsilon = 0$ (magenta), $\epsilon = 0.075$ (red), $\epsilon = 0.1$ (blue), $\epsilon = 0.25$ (orange), $\epsilon = 0.225$ (aqua), $\epsilon = 0.25$ (dark green), $\epsilon = 3$ (stars) and $\epsilon = 4$ (black)

can certainly determine the value one map by knowing the other. It also makes sense that the mutual information for the chaotic maps should be close to zero because they are chaotic.

To estimate the *mutual information* with binning, we produced values that could be binned by multiplying each population size by 100 and rounding to the nearest integer. Then we used the JIDT AutoAnalyzer [2] to compute the mutual information assuming discrete data. To generate figure 1 we used Matlab with the logistic map equation from [3].

To test whether the binning of the continuous data might be adversely affecting our estimation of mutual information, we also tried JIDT's kernel estimator to estimate the mutual information. In *kernel density estimation* (KDE), a Gaussian (bell) curve is centered at each data point. These Gaussian curves are collected, aggregated and finally normalized so that they integrate to one. The result is a smooth continuous estimate of the probability density, given only a finite amount of data[4]. One can then use the JIDT AutoAnalyzer to calculate the mutual information between the distributions. Under this method, we found the mutual information to be 1.7086 for the periodic maps, and 0.7192 for the chaotic maps. This reinforces what we see in Figure 1 because the chaotic maps have less mutual information than the periodic ones.

B. The Walker Model

For this project, we used the toy model of coupled logistic growth defined in [1]. This model uses the logistic map on a lattice of populations coupled with influence from the dynamics of the mean-field. For each time step n, the size of population i at time step n is defined to be

$$x_{i,n+1} = (1-\epsilon) f_i(x_{i,n}) + \epsilon m_n, \quad (i = 1, 2, \ldots N) \tag{4}$$

Here N is the number of time steps, n is the current time step (or generation), and ϵ is the coupling strength of the model to the entire lattice of organisms. Here the the local growth dynamics of each population i is defined by

$$f_i(x_{i,n}) = r_i x_{i,n} \left(1 - \frac{x_{i,n}}{K}\right) \tag{5}$$

Here r_i is the reproductive fitness of population i and K is the carrying capacity. We model the state of the entire lattice at time n by an average of the states of all the populations. This is called the *instantaneous mean field*, defined to be

$$M_n = \frac{1}{N} \sum_{j=1}^{N} x_{j,n} \tag{6}$$

The dynamics of the mean-field, m_n, is a measure of how the individual populations are growing at any time-step n.

$$m_n = \frac{1}{N} \sum_{j=1}^{N} f_j(x_{j,n}) \tag{7}$$

The influence of m_i on the entire system is quantified by the parameter ϵ, the coupling strength.

For simulation, we fix the carrying capacity to be $K = 100$, and we simulate $N = 1000$ populations for ten-thousand time steps. For each population, we initialize $x_{i,0} = 1$ and we generate a fitness value r_i independently and uniformly on the interval $[3.9, 4.0]$. Figure 2 shows return maps for various values of the global coupling strength ϵ.

To build the return map, equations 4, 5, 6, and 7 were implemented in Python using Numpy [6] and Matplotlib [7]. The return map shows that when the coupling $\epsilon = 0$, (magenta) there is not much change in how the overall state of the

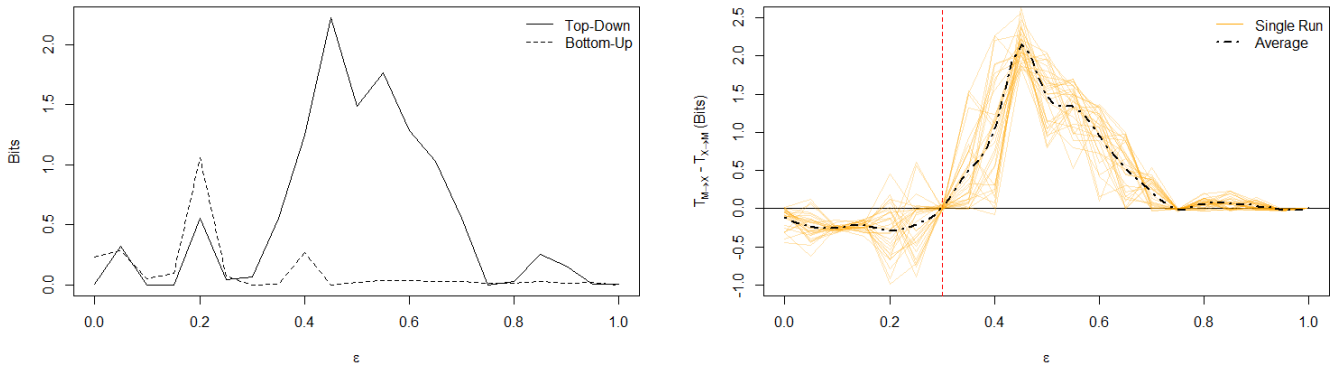

(a) (b)

Fig. 3. (a) Top-down, $T_{M\to X}$ (solid), and bottom-up, $T_{X\to M}$ (dashed), causal information transfer as a function of the global coupling parameter ϵ for coupled logistic maps. (b) The difference (Top-down minus bottom-up) in causal information transfer for 30 coupled systems as well as the mean as a function of ϵ (dashed). Vertical line at $\epsilon = 0.3$ illustrates the directional reversal of causal information transfer.

populations changes from time step to time step. That is, populations act independently of eachother. When $\epsilon > 0$, we see a variety of interesting behaviors.

It should be noted that the simulation is sensitive to the simulated fitness values r_i. In different runs of the return map, $\epsilon = 0.25$ (dark green) and and $\epsilon = 0.225$ (aqua) populations sometimes form loops. Moreover, there can be more than two attractors when $\epsilon = 0.3$. Overall, we see that coupling strengths $0, 0.075, 0.1$ and 0.4 produce consistently reproducible patterns, while there can be variation between runs in the regions produced by $\epsilon = 0.2, \epsilon = 0.225$ and $\epsilon = 0.3$.

While return maps that look like figure 2 seemed to occur more often, it would be interesting to look at the distributions of fitness values r_i that produce the more exotic return maps. This is beyond the scope of this paper.

C. Direction of Information Flow

In order to assess the direction of information flow from global to local scales and vice versa, the authors in [1] take advantage of *transfer entropy*. Transfer entropy is defined mathematically in [8] as

$$T^{(k)}_{Y\to X} = \sum_n p(x_{n+1}, x^{(k)}_n, y^{(k)}_n) \log \left[\frac{p(x_{n+1}|x^{(k)}_n, y^{(k)}_n)}{p(x_{n+1}|x_n(k)} \right]$$

Where $x^{(k)}_n$ is an embedded state in the k-dimensional phase space defined as $x^{(k)}_n = (x_n, \cdots, x_{n-k+1})$.

Although transfer entropy is a fine candidate for estimating the directionality of this coupling, recent work has focused on improving estimation methods. In their 2015 paper, Gencaga et. al propose new "statistically robust" methodology to estimate Transfer Entropy [9]. Relevant here is the considerable improvement for continuous processes, where discretizing the data can lead to a distortion in the underlying probability distribution. For this reason, we choose to use the state-of-the-art "Kraskov Estimtor", supported by the TransferEntropy[10] package in R, and claim based on this work that these estimates of transfer entropy are to be preferred for this problem.

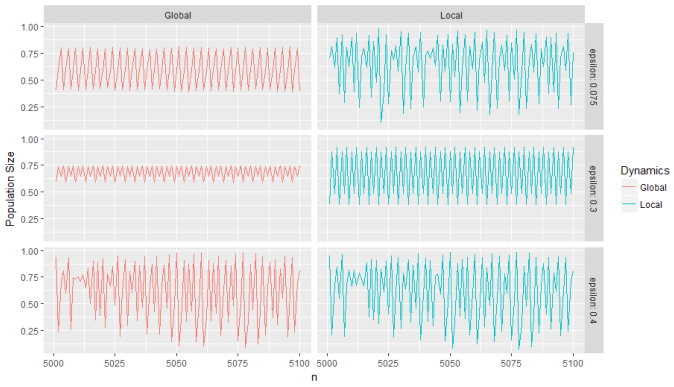

Fig. 4. Population trajectories for an individual (blue) and the mean (red) over 100 time steps. Dynamics are shown for $\epsilon = 0.075$ ($T_{X\to M} > T_{M\to X}$), $\epsilon = 0.3$ ($T_{X\to M} = 0 = T_{M\to X}$) and $\epsilon = 0.4$ ($T_{X\to M} < T_{M\to X}$.

In Figure 3a, we see qualitatively similar results as to what was demonstrated in [1]. The quantitative difference in the location and magnitude of the peaks can be attributed to either chance or estimation method. For low values of the global coupling parameter (ϵ), we see information flow is stronger in the bottom-down direction (from local to global scale). As ϵ increases, the direction reverses and top-down causation begins to dominate. We note again that we are qualitatively in agreement with the previous work [1]. There is however a subtle quantitative difference in our results. It appears from Figure 3a that this reversal of causation occurs at a value of $\epsilon = 0.3$. In an effort to analyze this claim

more rigorously, we repeat the entire simulation and estimation procedure 30 times. The right panel of Figure 3 shows the difference $T_{M\to X} - T_{X\to M}$ as a function of ϵ for 30 different simulations. The mean is also plotted, and we can see clearly that this reversal of information flow occurs right at $\epsilon = 0.3$. Finally, we note that this result is intuitively satisfactory since it coincides with the black stars in Figure 2, the value of ϵ for which the system is completely synchronized.

D. Additional Analysis

Here we continue our exploration of the relationship between local and global population dynamics. We will use the metric displayed in Figure 3, $T_{M\to X} - T_{X\to M}$, to discuss the direction of causal inforamtion transfer between the two scales. We break our discussion into 3 cases.

i) For small values of the global coupling strength, say $\epsilon < 0.3$, Figure 3 shows that our metric takes negative values. This indicates that causal information is flowing from the local to the global scale. The top row of Figure 4 shows that the individual population is chaotic, but the mean trajectory oscilates roughly between 3 values (0.4, 0.6 and 0.6). This is what gives the red points their behavior in Figure 2.

ii) For $\epsilon \approx 0.3$, the system synchronizes. In fact, we can compute the correlation between the trajectories in the middle row of Figure 4, and see that it is nearly equal to one (0.9879). Based on Figure 2 we sould expect these series to oscillate between precisely two values. This particular run had four attractors (black stars) instead of two.

iii) For large values of the global coupling strength, the global dynamics begin to dominate. There is still a near perfect correlation between M and X, but now even the global dynamics (the mean) behaves chaotically.

The mean-field only displays true near-periodic behavior when $\epsilon = 0.3$, when it oscilates between a small number of attractors. Although the mean population will never be truly asymptotic, it can be "pseudo-asymptotic". For instance when $\epsilon = 0$ and when $\epsilon = 0.1$, we see from Figure 2 that the mean-field bounces around a single attractor. For other values of ϵ, $\epsilon = 0.25$ and $\epsilon = 0.075$ in particular, the mean field bounces around in a "pseudo-periodic" fashion. When $\epsilon > 0.4$, we see that the mean-field is behaving chaotically itself.

We finish this section with a final discussion of the $\epsilon = 0.075$. In our example of Figure 4, we see that the individuals appear to be behaving nearly-chaotically, while the global trend oscilates roughly between 3 attracting regions. We argue that it is unlikely that top-down information transfer is driving this behavior. This is also coherent with our conclusions based on Figure 3, where we see that bottom-up information transfer is stronger for this value of ϵ.

III. Contributions

Each member of the team had an influence over all sections of this paper Precisely, Vanessa Job was the primary author of the introduction and the sections about figures 1 and 2, as well as the code that produced the the results in these sections. Kellin Rumsey was the primary author of the sections that produced figures 3 and 4, as well as the code that produced the results in these sections.

References

[1] Walker SI, Cisneros L, Davies PCW. 2012 Evolutionary transitions and top-down causation. *Proc. Artif Life* **XIII**, 283-290.

[2] Lizier, Joseph T. JIDT: An information-theoretic toolkit for studying the dynamics of complex systems, *Frontiers in Robotics and AI*, 1:11, 2014. [Online] https://github.com/jlizier/jidt

[3] M. Mitchell, Complexity. Oxford: Oxford University Press, 2011, pp. 27-37.

[4] Moon, Young-Il, Balaji Rajagopalan, and Upmanu Lall. Estimation of mutual information using kernel density estimators. *Physical Review E*, Volume 52, Number 3, September 1995.

[5] G. Flake, The computational beauty of nature. Cambridge, Mass.:*The MIT Press*, 2011, pp. 139-151.

[6] Stefan van der Walt, S. Chris Colbert and Gael Varoquaux. The NumPy Array: A Structure for Efficient Numerical Computation, *Computing in Science and Engineering,* 13, 22-30 (2011),

[7] Hunter, J.D. Matplotlib: A 2D graphics environment. *Computing in Science and Engineering*, Vol. 0, Num. 3, pp 90-95. (2007)[Online] Available: https://matplotlib.org

[8] Schreiber, T. (2007) Meausring information transfer. *Phys. Rev. Lett.*, 85:461

[9] D. Gencaga, K. H. Knuth, and W. B. Rossow, A recipe for the estimation of information flow in a dynamical system *Entropy* 17, 438 (2015)

[10] G. H. Torbati, G. Lawyer, TransferEntropy: The Transfer Entropy Package. R package, Version 1.4